

12 LEVEL III

AD

AD-E400 430

ADA 086093

TECHNICAL REPORT ARSCD-TR-80005

THERMOCHEMICAL AND BURNING RATE  
PROPERTIES OF  
DETERRED US SMALL ARMS PROPELLANTS

LUDWIG STIEFEL

DTIC ELECTE  
S JUL 2 1980 D  
B

JUNE 1980



US ARMY ARMAMENT RESEARCH AND DEVELOPMENT COMMAND  
 ✓ FIRE CONTROL AND SMALL CALIBER  
 WEAPON SYSTEMS LABORATORY  
 DOVER, NEW JERSEY

DDC FILE COPY.

APPROVED FOR PUBLIC RELEASE; DISTRIBUTION UNLIMITED.

80 6 23 025

The views, opinions, and/or findings contained in this report are those of the author(s) and should not be construed as an official Department of the Army position, policy or decision, unless so designated by other documentation.

Destroy this report when no longer needed. Do not return to the originator.

Any citation in this report to the names of commercial firms or commercially available products or services does not constitute official endorsement or approval of such commercial firms, products, or services by the United States Government.

UNCLASSIFIED

SECURITY CLASSIFICATION OF THIS PAGE (When Data Entered)

REPORT DOCUMENTATION PAGE		READ INSTRUCTIONS BEFORE COMPLETING FORM	
1. REPORT NUMBER Technical Report ARSCD-TR-80005	2. GOVT ACCESSION NO. AD-A086 093	3. RECIPIENT'S CATALOG NUMBER	
4. TITLE (and Subtitle) Thermochemical and Burning Rate Properties of Deterred U.S. Small Arms Propellants		5. TYPE OF REPORT & PERIOD COVERED Final	
		6. PERFORMING ORG. REPORT NUMBER	
7. AUTHOR(s) Ludwig Stiefel		8. CONTRACT OR GRANT NUMBER(s)	
9. PERFORMING ORGANIZATION NAME AND ADDRESS ARRADCOM, FC&SCWSL Armament Division (DRDAR-SCA-TC) Dover, NJ 07801		10. PROGRAM ELEMENT, PROJECT, TASK AREA & WORK UNIT NUMBERS 1L162617 AH19 TA06	
11. CONTROLLING OFFICE NAME AND ADDRESS ARRADCOM, TSD STINFO (DRDAR-TSS) Dover, NJ 07801		12. REPORT DATE June 1980	
		13. NUMBER OF PAGES 51	
14. MONITORING AGENCY NAME & ADDRESS (if different from Controlling Office)		15. SECURITY CLASS. (of this report) Unclassified	
		15a. DECLASSIFICATION/DOWNGRADING SCHEDULE	
16. DISTRIBUTION STATEMENT (of this Report)  Approved for Public Release; distribution unlimited.			
17. DISTRIBUTION STATEMENT (of the abstract entered in Block 20, if different from Report)			
18. SUPPLEMENTARY NOTES			
19. KEY WORDS (Continue on reverse side if necessary and identify by block number)  Propellants Small arms propellants Deterrents Burning rate Thermochemistry			
20. ABSTRACT (Continue on reverse side if necessary and identify by block number)  The depth of deterrent penetration was determined in eight U.S. military small arms propellants. The measurements were made on microtomed sections of the propellants. Staining techniques were used with some of the propellants to obtain good delineation of the deterrent-layer boundary. The propellants involved were double-base ball propellants WC 846 and WC 870, and single-base extruded IMR 4227, IMR 4350, IMR 5010, IMR 8138M, and CMR 160.			

DD FORM 1 JAN 73 1473

EDITION OF 1 NOV 65 IS OBSOLETE

UNCLASSIFIED

SECURITY CLASSIFICATION OF THIS PAGE (When Data Entered)

UNCLASSIFIED

SECURITY CLASSIFICATION OF THIS PAGE(When Data Entered)

20. ABSTRACT (Continued)

From the results of the depth of penetration measurements, the compositions of the inner, undeterred, region and the composition of the outer, deterrent-containing, region were calculated. The Hirshfelder-Sherman method and the BLAKE code were used to compute the thermochemical properties of the overall compositions, and the compositions of the deterred and undeterred regions. The results from the two approaches are compared.

The burning rate parameters were finally calculated for the different layers in the WC 870 and CMR 160 propellants on the basis of four different correlations of burning rate with adiabatic flame temperature. The results provide a selection of empirical equations to calculate burning rate constants, for the deterrent-containing and undeterred layers useful for interior ballistic calculations.

UNCLASSIFIED

SECURITY CLASSIFICATION OF THIS PAGE(When Data Entered)

ACKNOWLEDGMENT

The helpful suggestions and valuable assistance of Neil Lampner, FC&SCWSL, with microtoming and photomicrography, and the advice and assistance of Dr. Eli Freedman of the Ballistic Research Laboratories with the BLAKE code calculations are hereby gratefully acknowledged.

ACCESSION for		
NTIS	White Section	<input checked="" type="checkbox"/>
DDC	Buff Section	<input type="checkbox"/>
UNANNOUNCED		<input type="checkbox"/>
JUSTIFICATION _____		
BY _____		
DISTRIBUTION/AVAILABILITY CODES		
Dist.	AVAIL.	and/or SPECIAL
A		

## TABLE OF CONTENTS

	Page No.
Introduction	1
Experimental	3
Materials	3
Measurements	3
Results	7
Thermochemical Calculations	12
Burning Rate Estimation	21
Conclusions	32
Recommendations	36
References	36
Appendix	39
Distribution List	43

TABLES

		Page No.
1	Propellants used in this study and their applications	4
2	Chemical composition of the propellants	5
3	Granulation of the propellants	6
4	Depth of penetration of deterrent	11
5	Values for calculating $D_o^{(S)}$ , WC 846	14
6	Overall composition of WC 846, Lot BAJ 45608 and the composition of the deterred and undeterred regions	17
7	Overall composition of WC 870, Lot A.L. 45137 and the compositions of the deterred and undeterred layers	17
8	Overall compositions of the extruded propellants and the composition of the deterred and undeterred layers (IMR 4227, IMR 4350, IMR 8138M)	18
9	Overall compositions of the extruded propellants and the composition of the deterred and undeterred layers (IMR 4895, IMR 5010, CMR-160)	19
10	Percentage of propellant grain volume occupied by the deterrent-containing region	20
11	Results of thermochemical calculations with the Blake code and the Hirshfelder Method	22
12	Comparison of linear burning rates as estimated by various methods, at 68.94 MPa (10 Kpsi) and 137.9 MPa (20 Kpsi)	34

## FIGURES

	Page No.
1 Concentration profile of interacting plasticizer diffusing into polymer matrix	2
2 Photomicrographs of sections of WC 870 and WC 846 ball propellants	8
3 Photomicrographs of sections of IMR 4227, IMR 4350, and IMR 4895 propellants	9
4 Photomicrographs of sections of IMR 5010 and CMR 160 propellants	10
5 Geometry of a rolled-ball grain	13
6 Correlation of burning rate with flame temperature, Riefler and Lowry data	33

## INTRODUCTION

A need has been frequently expressed for quantitative data on the depth of penetration of deterrent coatings on the propellants used in the current small caliber cartridges. Such data are required as inputs for interior ballistic computer programs that deal explicitly with the characteristics of the deterred layer. Although such programs have been developed, their use is severely limited because of the lack of reliable input data, especially those data dealing with the outer regions of the propellant grains that have been impregnated with deterrent (ref 1). Data on the deterred layer are also needed in the analysis of pressure-time curves from closed-bomb firings that were conducted to investigate the burning behavior of consolidated charges (ref 2). Similarly, other interior ballistic efforts aimed toward defining the ignition and combustion processes occurring in small caliber charges depend on knowledge of characteristics of the deterred layer (ref 3).

The depth of penetration of the deterrent, its chemical identity, and its concentration level in the propellant are believed to characterize the deterred region from a chemical point of view for purposes of interior ballistic calculations (ref 4). The reason that the depth of penetration and the concentration of deterrent in the total propellant composition are considered sufficient to chemically characterize the deterred layer is due to the special shape of the concentration profile of the deterrent in propellant grains.

The deterrent concentration profile has been determined to have the shape depicted in figure 1 extracted from reference 5. The figure shows the shape of a diffusion front of a given plasticizer into a polymer matrix. This shape indicates that the deterrent concentration is nearly constant in the deterred layer and falls off sharply at the boundary line. The shape is attributed to the interaction between the plasticizer (i.e., the deterrent) and the polymer (i.e., nitrocellulose) (ref 6).

Microscopic studies of microtomed sections as well as autoradiographic studies of the concentration profile of di-n-butyl phthalate (DBP) in double-base ball propellants have confirmed the shape of figure 1 for ball propellants (refs 7, 8, 9). These studies also indicated that the depth of penetration observed with the optical microscope corresponds to the actual depth.

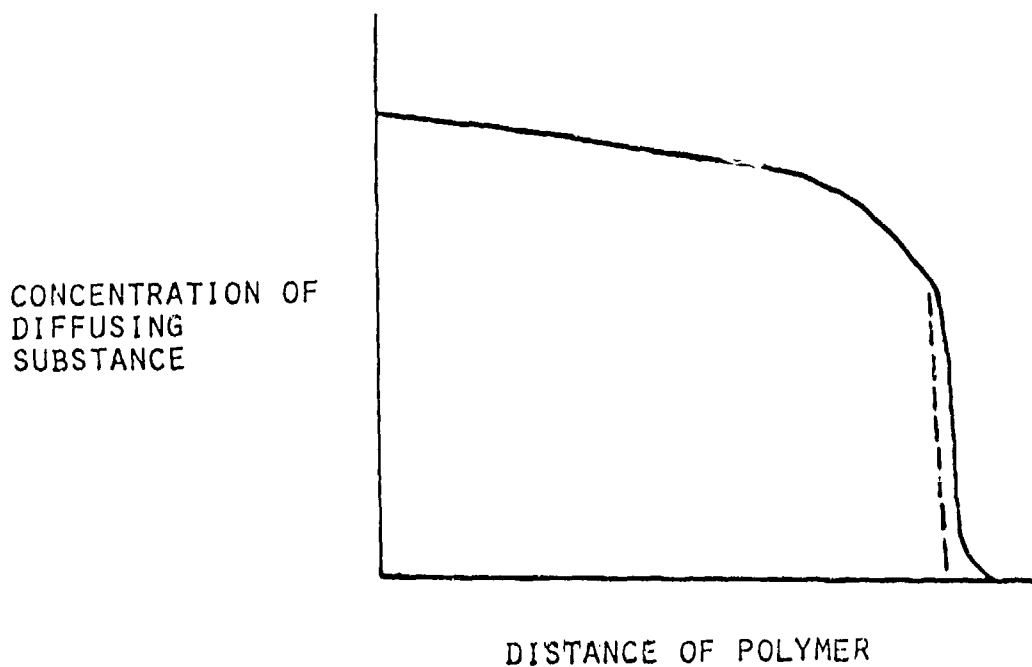


Figure 1. Concentration profile of interacting plasticizer diffusing into polymer matrix.

As a result of an extensive study of the diffusion of DBP into double-base ball propellants, a method for calculating the depth of penetration for ball propellants was developed (ref 9). This method is based on the conclusion that the final concentration profile can be best explained by a diffusion with interaction mechanism.

Studies of the depth of penetration have also been done on single-base extruded and double-base extruded propellants by means of microscopic studies of microtomed sections (refs 10, 11). However, the specific materials studied were experimental propellants not used in current cartridges. An extensive study of the concentration gradient of extruded propellants deterred with camphor, diethyl phthalate, or ethyl centralite has been reported. The method used involved the extraction and subsequent chemical analysis of microtomed sections. Both gas chromatography and mass spectrometry were used in the analysis. The studies indicate that, as with

ball propellants, the shape of the deterrent gradient is as depicted in figure 1 (ref 12). Consequently, in this study, the assumption is that the shape of the concentration profile of the deterrent resembles figure 1 for extruded propellants.

The consequence of a square-wave deterrent concentration profile is that one can assume a constant level of deterrent in the deterred region and that all of the deterrent in the propellant is evenly distributed through the deterred region. Furthermore, one can confidently use optical means for measuring the depth of penetration.

From the depth of penetration data, one can calculate the composition of the deterrent-containing region and the composition of the undeterred region from the known overall compositions. Once the compositions are known, one can obtain the thermochemical properties. In this study, two computational approaches were used, the Hirschfelder-Sherman method and the BLAKE code.

In addition to the thermochemical data, knowledge of the burning rate behavior of the propellants, as a function of pressure, is required input for the more advanced small arms interior ballistics calculations. For DBP deterred, double-base, ball propellants, the burning rate versus pressure relationship of the deterred layer can be obtained from the concentration of dibutyl phthalate, nitroglycerin, and nitrocellulose in that layer. This was made possible as a result of extensive closed-bomb studies aimed toward establishing the relationship between the chemical composition of various layers in ball propellants and their burning rate behavior (ref 13). A simplified approach had been proposed previously and this approach includes a means for dealing with the grain size distribution found in ball propellants (ref 4).

## EXPERIMENTAL

### Materials

The propellants selected for this effort are listed in table 1 along with some of the cartridges in which they are used. The propellants are representative of double-base ball propellants and of single-base extruded propellants coated with either dinitrotoluene, ethylene dimethacrylate, or methyl centralite.

### Measurements

The propellant grains were mounted on ceramic insulator rods approximately 3.2mm in diameter with Titebond Glue (Franklin Glue Co.). Thin sections, 20 to 30 $\mu$  thick, were then made with a sliding microtome.

Table 1. Propellants used in this study and their applications.

<u>Propellant Designation<sup>a</sup></u>	<u>Cartridge Type</u>
WC 846	7.62 mm NATO, Match 118 Ball M80 Tracer M62 AP M61 Ball M59 Reference (5.56 mm Ball M193) <sup>b</sup> .
WC 870	20 mm HPT M54A1 HEI M56A3.
IMR 4227	Not used in current military cartridges. Used in experimental caseless and consolidated charge munitions.
IMR 4350	Closed-bomb standard.
IMR 8138M	Not used in current military cartridges. Had been used in 7.62 mm NATO, Ball M80.
IMR 4895	Cal. .30 Match M72, API M14, grenade rifle M3, AP M2, Tracer M25, Ball M2, Reference, 7.62 mm NATO Match M118.
IMR 5010	Cal. .50 Tracer M17, M10, M1, Ball M33, APIT M20, API M8, AP M2.
CMR-160	Experimental double-base extruded propellant for 7.62 mm cartridges.

<sup>a</sup>The propellants used in this study, along with their chemical composition, are given in table 2. The grain dimensions of the extruded propellants or sieve-size distributions for the ball propellants are listed in table 3.

<sup>b</sup>Since 1971, the ball propellant used in this cartridge has been designated as WC 844 and is nearly identical to WC 846.

Table 2. Chemical composition of the propellants

Ingredient	WC 846 Lot BAJ45608	WC 870 Lot A.L.45137	IMR 4227 Lot 6217	IMR 4350 Lot 4047	IMR 8138N Lot RAD 44367	IMR 4895 Lot A.L. 41070	IMR 5010 Lot A.L. 29029	CMR-160 Lot Batch 1000
Nitrocellulose	81.40	79.70	89.72	91.56	92.96	88.99	88.27	95.77
(% nitrogen in NC)	(13.16)	13.11	13.15*	13.15*	13.15*	13.15*	13.15*	13.15*
Nitroglycerin	10.39	9.94	-	-	-	-	-	-
Dibutyl phthalate	5.61*	5.68*	-	-	-	-	-	-
Dinitrotoluene	0.06	0.69	6.74*	4.80*	-	7.55*	8.76*	-
Diphenylamine	0.97	0.95	0.84	0.85	0.89	0.78	0.55	0.73
Potassium nitrate	-	0.78	-	-	-	-	-	-
Potassium sulfate	-	-	0.73	0.73	0.69	0.93	0.64	0.84
Methylcentralite	-	-	-	-	-	-	-	2.43*
Ethylene dimethacrylate	-	-	-	-	3.60*	-	-	-
Total volatiles	1.23	1.26	1.60	1.72	-	-	1.78	1.63
Moisture	-	1.07	-	-	-	-	0.62	0.47
Graphite	0.12	0.10	0.37	0.33	0.11	0.22	0.1*	0.23
Calcium carbonate	0.09	0.79	-	-	-	-	-	-
Sodium sulfate	0.12	0.19	-	-	-	-	-	-
Tin dioxide	-	1.18	-	-	-	-	-	-

\* Deterrent coating

Table 3. Granulation of the propellants

Grain Dimensions	WC870		IMR 4227		IMR 4350		IMR 8138M		IMR 4895		IMR 5010		CMR-160
	Lot	Lot A.L.	Lot	Lot	Lot	Lot	Lot RAD	Lot A.L.	Lot A.L.	Lot A.L.	Lot A.L.	Lot	
	BAJ45608	45137	Lot 6217	Lot 4047	Lot 41070	29029	Batch 1000						
Length (mm)	0.559	2.108	1.092	1.435	2.040	1.374							
Outer diameter (mm)	0.584	0.965	.762	0.813	1.433	0.721							
Perf diameter (mm)	0.178	0.178	.178	0.178	.269	0.107							
Web (mm)	0.208	0.394	.279	0.318	.582	0.307							
Length (in.)	0.0220	0.0830	0.043	0.0565	0.0803	0.0541							
Outer diameter (in.)	0.023	0.038	0.030	0.032	0.0564	0.0284							
Perf Diameter (in.)	0.007	0.007	0.007	0.007	0.0106	0.0042							
Web (in.)	0.008	.0155	0.011	0.0125	0.0229	0.0121							

Sieve-size Distribution

Sieve No.	% Retained	
	WC 846	BAJ45608
U.S. #20	0.0	0.00
#25	1.1	3.24
#30	20.5	32.75
#35	25.0	52.14
#40	50.2	10.51
#45	2.8	1.02
PAN	0.2	0.21
		<u>0.94</u>
		99.91

\*Nominal

Measurements were made with a Leitz, Inc., Multipurpose, Measuring Microscope. This microscope is fitted with a digital micrometer, model 4098, and with a readout unit, model 1-525.5, both made by IKL, Inc. The unit provides automatic digital readout of measurements made with the microscope. A camera attachment with a polaroid pack affords the means for making the photomicrographs.

The deterred layer was readily evident in the ball propellants, i.e., in WC 846 and WC 870, and in IMR 8138M and IMR 5010. However, in the IMR 4227, IMR 4350, and IMR 4895, and in the CMR 160 propellants, the deterrent-containing regions were difficult to distinguish. Microtomed sections of those propellants were treated with an alcoholic solution of crystal violet as suggested by Quinlan (ref 10) to obtain sufficient contrast between the deterred and undeterred regions. All measurements and photomicrographs were made with a combination of incident and transmitted light.

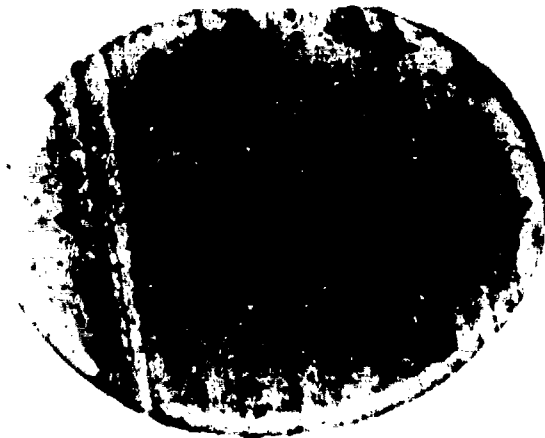
Five to ten grains were usually sectioned and five to ten sections were made from each grain. Since the thickness of the deterred layer often varied at different locations on the grain, the deterrent penetration was measured at a minimum of four locations to obtain measurements more representative of the grain as a whole.

#### RESULTS

Photomicrographs of sectioned grains of the various propellants are given in figures 2, 3, and 4. The results of depth of penetration measurements are given in table 4.

The mean depth of penetration of DBP in the WC 870 propellant (DBP concentration 5.68 percent) obtained in this study was 56.0 $\mu$  (0.0022 inch). This can be compared with results obtained by Brodman, et al. (ref 9) where WC 870 base grain propellant was used. For a DBP concentration of 5.17 percent, a depth of penetration of 42.2 $\mu$  (0.0017 inch) was reported. For a DBP concentration of 6.53 percent, a depth of penetration of 47.5 $\mu$  (0.0019 inch) was reported. The agreement of the results is satisfying in view of the fact that the propellants involved were not identical and that the deterring processes were somewhat different.

Small arms propellant lots are usually blends of two or more sublots. Blending is necessary because the quality of the product of the propellant manufacturing process is difficult to control to a high enough degree. In part, this difficulty arises from the major propellant ingredient, nitrocellulose, derived from a natural product, for example, wood pulp, whose quality varies. In addition, dimensional control of the grains and control of the deterrent level and depth of penetration are not sufficiently high.



WC 870 75.6X



WC 846 31.5X



WC 846 75.6X

Figure 2. Photomicrographs of sections of WC 870 and WC 846 ball propellants.



IMR 4227 75.6X



IMR 4350 75.6X



IMR 8138M 75.6X



IMR 4895 75.6X

Figure 3. Photomicrographs of sections of IMR 4227, IMR 4350, and IMR 4895 propellants.



IMR 5010 31.5X



CMR 160 75.6X

Figure 4. Photomicrographs of sections of IMR 5010 and CMR 160 propellants.

Table 4. Depth of penetration of deterrent

Propellant Designation	Propellant Type	Deterrent	Depth of Penetration, outer surface		Depth of penetration, perforation	
			Mean	Standard Deviation	Mean	Standard Deviation
WC 846	Double-base ball	DBP	0.0017	0.0003	-	-
			0.043	0.008	-	-
WC 870	Double-base ball	DBP	0.0022	0.0004	-	-
			0.056	0.010	-	-
IMR 4227	Single-base extruded	Dinitro-toluene	0.0011	0.0003	0.0011	0.0003
			0.028	0.008	0.028	0.0008
IMR 4350	Single-base extruded	Dinitro-toluene	0.0021	0.0004	0.0014	0.0003
			0.053	0.010	0.036	0.008
IMR 8138M	Single-base extruded	Ethylene Dimethacrylate	0.0019	0.0002	0.0017	0.0005
			0.048	0.005	0.043	0.013
IMR 4895	Single-base extruded	Dinitro-toluene	0.0014	0.0002	0.0013	0.0003
			0.036	0.005	0.033	0.008
IMR 5010	Single-base extruded	Dinitro-toluene	0.0050	0.0003	0.0023	0.0007
			0.127	0.008	0.058	0.018
CMR 160	Single-base extruded	Methyl Centralite	0.0018	0.0003	0.0015	0.0005
			0.046	0.008	0.038	0.013

Two or more different sublots of propellant are usually blended to meet ballistic performance requirements. Consequently, a given lot can contain grains from different base grain lots and from different coating runs with different deterrent levels and depths of penetration.

Industry practice is, at least with the propellants dealt with in this report, that materials are not blended which differ widely in ballistic behavior. Nevertheless, because small arms propellant lots are blends, no attempt was made to systematize the measurements in terms of the base grain composition or in terms of deterrent. Rather, the data on depth of penetration are presented in terms of the mean and standard deviation for use as computer input for interior ballistic calculations.

#### THERMOCHEMICAL CALCULATIONS

Once the depth of penetration is known, and using the overall composition of the propellant, one can calculate the compositions of the deterred and undeterred regions of small arms propellant grains. Furthermore, this then permits calculation of thermochemical data such as impetus and flame temperature for the separate regions. One can also estimate burning rate versus pressure parameters from these data using various empirical estimation techniques.

The procedure used in this study for calculating the composition of the deterrent-containing and undeterred region of the ball propellants is described first. The procedure is complicated by the fact that the ball propellant manufacturing process results in a fairly wide size distribution of particles that are more or less spherical. After the particles have been classified by sieving, those particles within a certain size range are deterrent coated. If the product is a rolled-ball propellant, the deterrent-coated particles are passed through rollers which transform the spherical particles into discs of uniform thickness. The larger particles are most severely distorted and may exhibit fissures or notches.

The procedure used to obtain the compositions of the deterred and undeterred regions of WC 846 propellant, which is a rolled-ball type, follows the model developed by Goldstein (refs 14, 15).

In these calculations, the following assumptions are made:

1. The grains have the form of discs with rounded edges and have a uniform thickness (see figure 5, which is taken from reference 15).

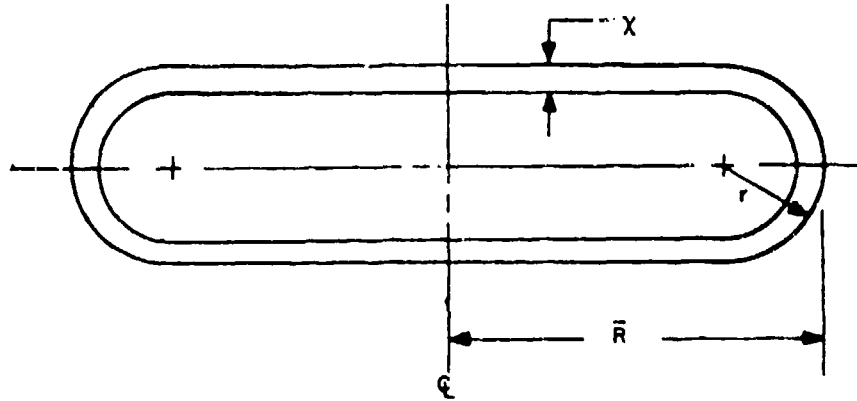


Figure 5. Geometry of a rolled-ball grain.

2. The deterrent concentration gradient is a step function, as in figure 1.

3. The nitroglycerin, which is diffused into the grain after formation of the spherical particles, is assumed to be uniformly distributed throughout the grain.

Since the particle size varies, the description of the grain geometry of a given ball propellant for purposes of interior ballistic calculations can be expressed as the equivalent mean diameter  $D_o^{(S)}$  based on particle surface area (ref 15).  $D_o^{(S)}$  is calculated from the following equation with the particle size distribution obtained from a sieve analysis of the propellant.

$$D_o^{(S)} = \left[ \frac{\sum_i (2R_i)^2 \frac{F_i}{V_i}}{\sum_i \frac{F_i}{V_i}} \right]^{1/2} \quad (1)$$

where,  $F_i = \frac{N_i V_i}{V_t}$

$\bar{R}_i$  = average radius of grains within a given sieve range.

$V_i$  = the initial volume of single grain of radius  $R_i$

$V_t$  = volume occupied by a unit weight of propellant

$N_i$  = number of grains having radius  $R_i$

Description sheets accompanying ball propellant lots usually give the sieve analysis results. The particle size distribution for WC 846, Lot BAJ 45608, used in this study, is given in table 3. Values used for calculating  $D_o^{(S)}$  for the propellant are given in table 5.

Table 5. Values for calculating  $D_o^{(S)}$  WC 846

$F_i$	U.S. Sieve No.	$L_i$ Sieve Opening (mm)	$\bar{L}_i^a$ (mm)	$\bar{R}_i^b$ (mm)	$\bar{V}_i^c$ (mm)
	20	.841			
.011	25	.707	.774	.4684	.2208
.205	30	.595	.651	.3814	.1396
.250	35	.500	.548	.3086	0.0879
.502	40	.420	.460	.2464	0.0527
.028	45	.354	.387	.1947	0.03045
.002	50	.297	.326	.1546	

a

$$\bar{L}_i = \frac{L_{i-1} + L_i}{2}$$

b

$$\bar{R}_i = \frac{\sqrt{2}}{2} \bar{L}_i - (\sqrt{2}r - r) \quad (2)$$

where  $r = \frac{\text{web}}{2} = \frac{0.381}{2} = 0.1905\text{mm}$

c

$$\bar{V}_i = \text{average volume of a rolled ball grain within a given sieve size range.}$$

The average volume of the rolled-ball grains is given by:

$$\bar{V}_o = 2\pi r (\bar{R}-r) \pi^2 r^2 \left[ (\bar{R}-r) + \frac{4}{3} \frac{r}{\pi} \right] \quad (3)$$

The value for  $D_o^{(S)}$  was obtained by inserting the appropriate number into equation 1. For the WC 846 propellant lot BAJ 45608,  $D_o^{(S)} = 0.5473$  mm.

If the depth of penetration of deterrent is  $x$ , the volume of the undeterred region  $V_{un}$  is:

$$V_{un} = 2\pi(\bar{R}-r)^2(r-x) + \pi^2(r-x)^2 \left[ (\bar{R}-r) + \frac{4(r-x)}{3\pi} \right] \quad (4)$$

The total grain volume  $\bar{V}_o$  was found to be  $0.0670 \text{ mm}^3$ , and the volume of the undeterred larger  $\bar{V}_{un}$  was found to be  $0.0381 \text{ mm}$  (ref 3). Then, the undeterred region occupies:

$$\frac{\bar{V}_{un}}{\bar{V}_o} \times 100 = 56.87\% \text{ of the volume of the grain.}$$

On the assumption that all of the deterrent, DBP, i.e., 5.28 percent (table 2) was located in the deterred region, the concentration of that region was found to be 12.24 percent. The composition of the deterred and undeterred regions was then calculated and is given in table 6 along with the overall composition given in table 2. Details of this part of the calculation are given in the appendix.

The values for moisture ( $H_2O$ ) and residual solvent have been arbitrarily taken to be equal to one-half of the total volatiles in the following tables. This was done because the reported values for moisture are obtained by empirical methods and the validity is questionable.

Calculation of the composition of the deterrent-containing and undeterred region of the spherical ball propellant (unrolled) WC 870 follows the same procedure, except that the geometry of the grain is assumed to be a sphere which simplifies the applicable equations (i.e., equations 2, 3, and 4) accordingly.

The weighted mean diameter based on surface area  $D_o^{(S)}$  of the grain of WC 870 Lot A.L. 45137 was found to be 0.7902 mm. The average grain volume,  $\bar{V}$ , was  $2.584 \times 10^{-4} \text{ cm}^3$ . The average volume of the undeterred region,  $\bar{V}_{un}$ , was found to be  $1.649 \times 10^{-4} \text{ cm}^3$  and the undeterred region in the WC 870 propellant was found to occupy 63.79 percent of the total volume of the grain. The compositions of the deterred and undeterred layers determined from these results are given in table 5.

The extruded propellants have a uniform grain geometry (i.e., single perforated cylinders) as given in table 3. Calculation of the composition of the deterred and undeterred regions for these propellants involves the following steps:

1. Calculate the volume of the total grain.
2. Calculate the volume of the deterred region using the measured depths of deterrent penetration in table 4.
3. Assuming that all of the deterrent is concentrated in the deterred region, calculate the concentration of the deterrent in that region. Then, obtain the concentrations of the other constituents.
4. Assuming total absence of the deterrent in the undeterred region, calculate its composition.

The results of these computations for the extruded propellants are given in tables 8 and 9, along with their overall chemical composition. For purposes of comparison, the percentage of the propellant grain volume, occupied by the deterrent-containing region for each of the propellants is listed in table 10.

Two methods were used for calculating the thermochemical properties associated with the compositions given in tables 6, 7, 8, and 9 were used. One of these was the Hirshfelder-Sherman Additive Constant method (ref 16). A computer program (ref 17) based on this method, was used for these calculations.

Table 6. Overall chemical composition of Wc 846. Lot BAJ 45608 and the composition of the deterred and undeterred regions

<u>Ingredient</u>	<u>Overall Composition(%)</u>	<u>Undeterred Layer (%)</u>	<u>Deterred Layer (%)</u>
Nitrocellulose	81.40	86.23	75.01
% nitrogen	(13.16)	(13.16)	13.16
Nitroglycerin	10.39	11.00	9.57
Dibutyl phthalate	5.61	0.00	13.01
Dinitrotoluene	0.06	0.06	0.05
Diphenylamine	0.97	1.03	0.90
Total volatiles			
- Water	0.62	0.66	0.57
- Ethyl acetate	0.61	0.65	0.57
Graphite	0.13	0.14	0.12
Calcium carbonate	0.09	0.10	0.09
Sodium sulfate	<u>0.12</u>	<u>0.13</u>	<u>0.11</u>
	100.00	100.00	100.00

Table 7. Overall composition of WC 870 Lot A.L. 45137 and the compositions of the deterred and undeterred layers

<u>Ingredient</u>	<u>Overall Composition (%)</u>	<u>Undeterred Layer (%)</u>	<u>Deterred Layer (%)</u>
Nitrocellulose	79.70	84.13	71.89
% nitrogen	(13.11)	(13.11)	(13.11)
Nitroglycerin	9.21	9.72	8.31
Dibutyl phthalate	5.27	0.0	14.55
Dinitrotoluene	0.64	0.68	0.58
Diphenylamine	0.88	0.93	0.79
Total volatiles	1.26	1.33	1.14
- Water	0.63	0.67	0.57
- Ethyl acetate	0.63	0.67	0.57
Graphite	0.10	0.11	0.09
Potassium nitrate	0.78	.82	0.70
Calcium carbonate	0.79	0.83	.71
Sodium sulfate	0.19	0.20	.17
Tin dioxide	<u>1.18</u>	<u>1.25</u>	<u>1.07</u>
	100.00	100.00	100.00

Table 8. Overall compositions of the extruded propellants and the composition of the deterred and undeterred layers (IMR 4227, IMR 4350, IMR 8138M)

Ingredient	IMR 4227, 6217			IMR 4350, 4047			IMR 8138M RAD 44367		
	Overall Comp. (%)	Undeterred Layer (%)	Deterred Layer (%)	Overall Comp. (%)	Undeterred Layer (%)	Deterred Layer (%)	Overall Comp. (%)	Undeterred Layer (%)	Deterred Layer (%)
Nitrocellulose	89.72	96.20	77.53	91.57	96.18	80.16	92.96	96.43	86.31
% nitrogen	13.15*	13.15*	13.15*	13.15*	13.15*	13.15*	13.15*	13.15*	13.15*
Dinitrotoluene	6.74	0.0	19.40	4.80	0.0	16.67			
Diphenvlamine	0.84	0.90	0.73	0.85	0.89	0.74	0.89	0.92	0.83
Potassium sulfate	0.73	0.78	0.63	0.73	0.77	0.64	0.69	0.72	0.65
Total volatiles									
- Water	0.80	0.86	0.70	0.86	0.91	0.75	0.88	0.91	0.83
- Ethyl alcohol	0.80	0.86	0.69	0.86	0.90	0.75	0.87	0.91	0.82
Graphite	0.37	0.40	0.32	0.33	0.35	0.29	0.11	0.11	0.10
Ethylene dimeth-acrylate							3.60	0.0	9.46

\*Nominal

Table 9. Overall compositions of the extruded propellants and the compositions of the deterred and undeterred layers (IMR 4895, IMR 5010, CMR-160)

Ingredient	IMR 4895			IMR 5010			CMR-160		
	Lot A.L. 41070			Lot. A.L. 29029			Lot Batch 1000		
	Overall Comp. (%)	Undeterred Layer (%)	Deterred Layer (%)	Overall Comp. (%)	Undeterred Layer (%)	Deterred Layer (%)	Overall Comp. (%)	Undeterred Layer (%)	Deterred Layer (%)
Nitrocellulose	88.99	96.26	68.7	88.23	96.70	78.01	94.08	96.39	89.38
% nitrogen	13.15*	13.15*	13.15*	13.15*	13.15*	13.15*	12.87	12.87	12.87
Dinitrotoluene	7.55	0.0	29.19	8.75	0.0	19.35	-	-	-
Methyl centralite	-	-	-	-	-	-	2.39	7.28	7.28
Diphenylamine	0.78	0.84	0.59	0.55	0.60	0.48	0.71	0.73	0.68
Potassium sulfate	0.93	1.02	0.72	0.64	0.70	0.57	0.82	0.84	0.77
Total volatiles	0.77	0.83	0.59	0.87	0.95	0.75	0.87	0.89	0.82
- Water	0.76	0.82	0.58	0.86	0.94	0.75	0.86	0.87	0.82
- Ethyl alcohol	0.22	0.23	0.16	0.11	0.11	0.09	0.26	0.27	0.25
Graphite									

\*Nominal

Table 10. Percentage of propellant grain volume occupied by the deterrent containing region.

<u>Propellant</u>	WC 846 Lot BAJ 45608	WC 870 Lot A.L. 45137	IMR 4227 Lot 6217
Volume per grain (cm <sup>3</sup> )	6.70x10 <sup>-5</sup>	2.584x10 <sup>-4</sup>	1.359x10 <sup>-4</sup>
Volume of deterred region (cm <sup>3</sup> )	2.89x10 <sup>-5</sup>	9.355x10 <sup>-5</sup>	4.725x10 <sup>-5</sup>
% Deterred volume	43.13	36.21	34.75

IMR 4350 Lot 4047	IMR 8138M Lot RAD 44367	IMR 4895 Lot A.L. 41070	IMR 5010 Lot A.L. 29029	CMR-160 Lot Batch 1000
1.491x10 <sup>-3</sup>	4.711x10 <sup>-4</sup>	7.091x10 <sup>-4</sup>	3.178x10 <sup>-3</sup>	5.494x10 <sup>-4</sup>
4.291x10 <sup>-4</sup>	1.792x10 <sup>-4</sup>	1.834x10 <sup>-4</sup>	1.439x10 <sup>-3</sup>	1.833x10 <sup>-4</sup>
28.79	38.05	25.87	45.28	33.86

The Hirshfelder-Sherman method, although relatively primitive, has been widely used in the gun propellant field for many years, and considerable confidence has been established for it. The other method involved the use of the BLAKE code developed by Freedman (ref 13). This code is an advanced chemical equilibrium program especially formulated for gun ballistic purposes.

To permit ready comparison of the results from the two methods required a number of minor modifications to the compositions in tables 6 to 7. As mentioned before, the total volatiles were assumed to consist of 50 percent moisture (H<sub>2</sub>O) and 50 percent residual solvent. For the extruded propellant, the residual solvent was assumed to be ethyl acetate. The data bases for both codes did not contain data to permit input of compositions containing sodium sulfate, tin dioxide, or calcium carbonate. Consequently, those compounds, which when present, were there in relatively small amounts, were lumped, and considered as potassium sulfate in the calculations\*. The calculations made with the BLAKE code were done for a loading density of 0.2 g/cc.

\*Strictly speaking, sodium sulfate could be handled by the BLAKE code; but, to permit direct comparison of the results, the same input compositions were used with both codes.

The results of the computations are given in table 11. Agreement between the two methods was found to be very good in most instances. The largest differences in calculated flame temperature between the BLAKE code and the Hirschfelder method occurred with compositions having very low flame temperatures (i.e., deterred WC 870,  $T_v = 2081$ , 1978).

The Hirschfelder method is based on estimates of the properties of the product species over a temperature range found in the common World War II propellants. This method, thus, is probably less valid with materials that fall too far outside of that range.

#### BURNING RATE ESTIMATION

The linear burning rate of propellants as a function of pressure is commonly described for interior ballistics calculation by means of an equation of the following form:  $r = bP^n$ , known as the De Saint Robert equation (ref 21).

Experience has indicated that the linear burning rate of a propellant increases with the flame temperature. This observation has led to suggestions for empirical correlations between the flame temperature of propellant compositions and their burning rate parameters (i.e.,  $b$  and  $n$ ) in the above equation ( $r = bP^n$ ).

The availability of flame temperature values for both the deterrent-containing layer and the undeterred layer provided an opportunity to determine the burning rate parameters for the various compositions. Furthermore, these values provided an opportunity to compare the various methods for estimating the burning rate of gun propellants.

Table 11. Results of thermochemical calculations with the BLAKE code and the Hirshfelder method

	T <sub>v</sub> (°K)	Pressure		Impetus $\frac{\text{ft-lb}}{\text{lb}}$	n $\frac{\text{g-moles}}{\text{g}}$	Ratio of Specific heats		Covolume $(\text{cc/g}) (\text{in.}^3/\text{lb})$	
		(MPa)	(Kpsi)			(J/g)	$\gamma$		
<u>WC 846 Overall Composition</u>									
BLAKE	2855	255.9	37.11	1011.1	338,300	.0426	1.2461	1.048	29.02
Hirshfelder	2813	-	-	997.4	333,700	.0426	1.243	.934	25.86
<u>WC 846 Undeterred Composition</u>									
BLAKE	3343	273.5	39.66	1095.3	366,400	.0394	1.226	0.995	27.54
Hirshfelder	3268	-	-	1071.1	358,300	.0394	1.227	0.906	25.07
<u>WC 846 Deterred Composition</u>									
BLAKE	2244	224.1	32.50	867.7	290,300	.0465	1.273	1.128	31.21
Hirshfelder	2193	-	-	855.7	286,300	.0469	1.263	0.972	26.90

Table 11. (Continued)

	T <sub>v</sub> (°K)	Pressure		Impetus $\frac{\text{ft-lb}}{\text{lb}}$	n $\frac{\text{g-moles}}{\text{g}}$	Ratio of Specific heats		Covolume $(\text{in.}^3/\text{lb})$	
		(MPa)	(Kpsi)			$\gamma$	$\gamma$		
<u>WC 870 Overall Composition</u>									
BLAKE	2782	243.6	35.33	967.6	323,700	0.0418	1.246	1.027	28.43
Hirshfelder	2750	-	-	954.8	319,300	0.0416	1.241	0.930	25.85
<u>WC 870 Undeterred Composition</u>									
BLAKE	3216	258.6	37.51	1039.8	347,900	0.0389	1.227	0.979	27.10
Hirshfelder	3189	-	-	1025.1	343,060	0.0385	1.227	0.907	25.11
<u>WC 870 Deterred Composition</u>									
BLAKE	2081	205.6	29.82	796.3	266,400	.0457	1.277	1.126	31.18
Hirshfelder	1978	-	-	775.6	259,500	.0470	1.266	0.981	27.15

Table 11. (Continued)

	T <sub>v</sub> (°K)	Pressure		Impetus $\frac{\text{ft-lb}}{\text{lb}}$	n $\frac{\text{g-moles}}{\text{g}}$	Ratio of Specific heats		Covolume (cc/g) (in. <sup>3</sup> /lb)	
		(MPa)	(Kpsi)			γ	γ		
<u>IMR 4227 Overall Composition</u>									
BLAKE	2878	252.7	36.65	1000.7	334,800	.0418	1.245	1.040	28.79
Hirshfelder	2847			989.4	331,000	.0418	1.242	0.936	25.90
<u>IMR 4227 Undeterred Region</u>									
BLAKE	3048	257.4	37.33	1026.6	343,500	.0405	1.235	1.011	27.98
Hirshfelder	3008			1012.0	338,600	.0404	1.233	0.917	25.38
<u>IMR 4227 Deterred Region</u>									
BLAKE	2550	240.6	34.90	938.2	313,900	.0442	1.264	1.101	30.47
Hirshfelder	2537			935.3	312,900	.0443	1.259	0.971	26.86

Table 11. (Continued)

	TV (°K)	Pressure		Impetus $\frac{\text{ft-lb}}{\text{lb}}$	n $\frac{\text{g-moles}}{\text{g}}$	Ratio of Specific heats		Covolume $(\text{in.}^3/\text{lb})$	
		(MPa)	(Kpsi)			(J/g)	$\gamma$		(cc/g)
<u>IMR 4350 Overall Composition</u>									
BLAKE	2927	254.2	36.87	1009.0	337,600	.0415	1.242	1.031	28.55
Hirshfelder	2893	-	-	996.6	333,400	.0414	1.239	0.930	25.73
<u>IMR 4350 Undeterred Composition</u>									
BLAKE	3048	257.4	37.33	1026.8	343,500	.0405	1.235	1.010	27.96
Hirshfelder	3008	-	-	1012.1	338,600	0.0404	1.233	0.917	25.37
<u>IMR 4350 Deterred Composition</u>									
BLAKE	2622	243.7	35.35	953.7	319,000	.0437	1.260	1.087	30.08
Hirshfelder	2605	-	-	948.8	317,400	0.0438	1.255	0.963	26.64

Table 11. (Continued)

	Temperature		Pressure		Impetus ft-lb lb	n g-moles g	Ratio of Specific heats		Covolume (cc/g) (in. <sup>3</sup> /lb)
	T <sub>v</sub> (°K)	(°K)	(MPa)	(Kpsi)			γ	γ	
<u>IMR 8138M Overall Composition</u>									
BLAKE	2816	248.2	36.00	984.5	329,400	.0420	1.245	1.034	28.62
Hirshfelder	2770	-	-	968.4	324,000	0.0420	1.240	0.929	25.70
<u>IMR 8138M Undeterred Composition</u>									
BLAKE	3068	258.6	37.50	1032.2	345,300	.0405	1.234	1.008	27.91
Hirshfelder	3028	-	-	1017.3	340,400	0.0404	1.232	0.915	25.32
<u>IMR 8138M Deterred Composition</u>									
BLAKE	2406	227.7	33.02	892.1	298,500	0.0446	1.263	1.081	29.93
Hirshfelder	2358	-	-	876.2	293,200	0.0447	1.252	0.951	26.32

Table 11. (Continued)

	TV (°K)	Pressure		Impetus (J/g)	ft-lb lb	n g-moles g	Ratio of Specific heats		Covolume (cc/g) (in. <sup>3</sup> /lb)
		(MPa)	(Kpsi)				γ	γ	
<u>IMR 4895 Overall Composition</u>									
BLAKE	2874	252.2	36.57	998.7	334,100	0.0418	1.245	1.039	28.77
Hirshfelder	2845	-	-	988.1	330,600	0.0417	1.242	0.936	25.91
<u>IMR 4895 Undeterred Composition</u>									
BLAKE	3067	257.3	37.31	1027.6	343,800	0.0403	1.234	1.006	27.84
Hirshfelder	3028	-	-	1013.0	338,900	0.0402	1.232	.915	25.33
<u>IMR 4895 Deterred Composition</u>									
BLAKE	2287	226.2	32.80	870.8	291,300	0.0458	1.278	1.150	31.80
Hirshfelder	2310	-	-	886.1	296,500	0.0461	1.272	.996	27.57

Table 11. (Continued)

	TV (°K)	Pressure		Impetus $\frac{\text{ft-lb}}{\text{lb}}$	n g-moles g	Ratio of Specific heats		Covolume (cc/g) (in. <sup>3</sup> /lb)	
		(MPa)	(Kpsi)			Y	γ		
<u>IMR 5010 Overall Composition</u>									
BLAKE	2869	253.3	36.73	1002.0	335,200	0.0420	1.246	1.043	28.88
Hirshfelder	2840	-	-	991.8	331,800	0.0420	1.243	0.937	25.93
<u>IMR 5010 Undeterred Composition</u>									
BLAKE	3094	259.3	37.61	1036.1	346,600	0.0403	1.233	1.004	27.80
Hirshfelder	3052	-	-	1020.9	341,600	0.0402	1.231	0.912	25.25
<u>IMR 5010 Deterred Composition</u>									
BLAKE	2593	243.2	35.27	949.6	317,700	0.0440	1.262	1.095	30.30
Hirshfelder	2580	-	-	946.4	316,700	0.0441	1.257	0.967	26.75

Table 11. (Continued)

	T <sub>v</sub> (°K)	Pressure		Impetus $\frac{\text{ft-lb}}{\text{lb}}$	n g-moles g	Ratio of Specific heats $\gamma$	Covolume (cc/g) (in. <sup>3</sup> /lb)		
		(MPa)	(Kpsi)						
<u>CMR 160 Overall Composition</u>									
BLAKE	2776	246.1	35.96	974.6	326,100	0.0422	1.247	1.039	28.77
Hirshfelder	2731	-	-	957.8	320,500	0.0419	1.242	0.932	25.78
<u>CMR 160 Undeterred Region</u>									
BLAKE	2973	253.3	36.74	1009.9	337,900	0.0408	1.237	1.013	28.04
Hirshfelder	2950	-	-	996.9	333,500	0.0404	1.233	0.914	25.23
<u>CMR 160 Deterred Region</u>									
BLAKE	2373	227.5	33.00	887.2	296,800	0.0450	1.267	1.100	30.46
Hirshfelder	2338	-	-	876.4	293,200	0.0448	1.257	0.963	26.66

Four correlations were compared in this study as follows:

Grollman and Nelson (ref 19):

$$b = (T-1800)(1.65 \times 10^{-7})(n^{-9.4}); \quad r = \text{in./s}, \quad p = \text{psi}$$

$$b = (T-1800)(4.19 \times 10^{-6})(145^n)(n^{-9.4}); \quad r = \text{mm}, \quad p = \text{MPa}$$

where T is the adiabatic, isochoric flame temperature.

Muraour (ref 20):

$$r = 0.2 + 0.0000212e^{0.709(T/1000)} p; \quad r = \text{in./s}, \\ p = \text{psi}$$

$$r = 0.5 + 0.078e^{0.709(T/1000)} p; \quad r = \text{mm/s}, \\ p = \text{MPa}$$

Goldstein (ref 15)\*:

$$b = e^{-8.15 + 8.62 \times 10^4 T_v}$$

$$r = \text{in/sec}, \quad p = \text{psi}, \quad n = 0.7$$

$$b = e^{-8.15 + 8.62 \times 10^{-4} T_v} (8.2776 \times 10^2) \quad n = 0.7$$

where  $r = \text{mm/s}$ ,  $p = \text{MPa}$

\*NOTE: The following two equations must be used with the pressure exponent,  $n = 0.7$

Riefler and Lowery (ref 13):

This correlation is not analogous to the previous three. It is a direct correlation of burning rate of ball propellants as a function of their nitroglycerin and dibutyl phthalate content. It is further discussed in this section.

The estimation methods were evaluated at four flame temperatures. The temperatures selected were those for the deterrent-containing and undeterred layers of WC 870 and CMR-160.

The Riefler and Lowery (ref 13) burning rate correlation was based on closed-bomb burning rate measurements of a series of sixteen propellants with flame temperatures varying between 1802°K and 3131°K and, as explained above, permits the direct calculation of the burning rate parameters b and n from the percentage of dibutyl phthalate (DBP) and nitroglycerin (NG).

Two models are offered by Riefler and Lowery (ref 13), a constant coefficient model and a constant exponent model. The constant exponent model is:

$$r = e^{-(-6.61872) + (\%DBP)(-0.052882) + (\%NG)(0.015970)} p^{0.8053}$$

where

$$r = \text{in./s}, \quad p = \text{psi}$$

In metric units:

$$r = (1.390 \times 10^3) e^{-(-6.61872) + (\%DBP)(-0.052882) + (\%NG)(0.015907)} p^{0.8053}$$

where

$$r = \text{mm/s} \quad p = \text{MPa}$$

In the present study, a further correlation of the flame temperature versus the burning rate coefficient was made with the Riefler and Lowery experimental data. A constant exponent (n = 0.8053) was assumed.

A least-squares method was used to fit the flame temperature and burning rate coefficient data (constant exponent, n = 0.8053). The best fit was obtained with a linear equation as follows:

$$b = -0.0006 + 0.064 \times 10^{-6} T_v$$

where

$$r = \text{in./s}, \quad P = \text{psi}, \quad n = 0.8053$$

and

$$b = -0.8340 + 8.3956 \times 10^{-4} T_v$$

where

$$r = \text{mm/s}, \quad p = \text{MPa}, \quad n = 0.8053$$

A plot of the burning rate coefficient versus flame temperature with Riefler and Lowery data is given in figure 6 and shows the best fit straight line.

A comparison of results obtained when burning rates are calculated by the two Riefler and Lowery correlations. The results based on the NG, DBP correlation are given in column A, table 12. The calculation was made possible because the 3200°K and 2000°K propellants correspond with the two regions in the WC 870 ball propellant. The values obtained by use of the direct correlation of  $b$  versus  $T_v$  carried out in this study given in column B. The agreement with the other values is quite satisfactory.

The largest discrepancy in the estimated values occurs with a low flame temperature in the Grollman & Nelson correlation probably because the Grollman & Nelson correlation was based only on conventional gun propellant data, none of which had flame temperatures under 2400°K.

#### CONCLUSIONS

1. Measurements of the depth of deterrent penetration were made for eight small arms propellants.
2. The compositions of the deterrent-containing layer and that of the undeterred region were calculated.
3. The thermochemical data required for interior ballistic calculations were computed by means of the Hirschfelder-Sherman method and by means of the BLAKE code.
4. The results of the thermochemical calculations with the Hirschfelder-Sherman method and the BLAKE code are in good agreement. The largest differences occurred with formulations having very low flame temperatures (i.e., 2100°K).

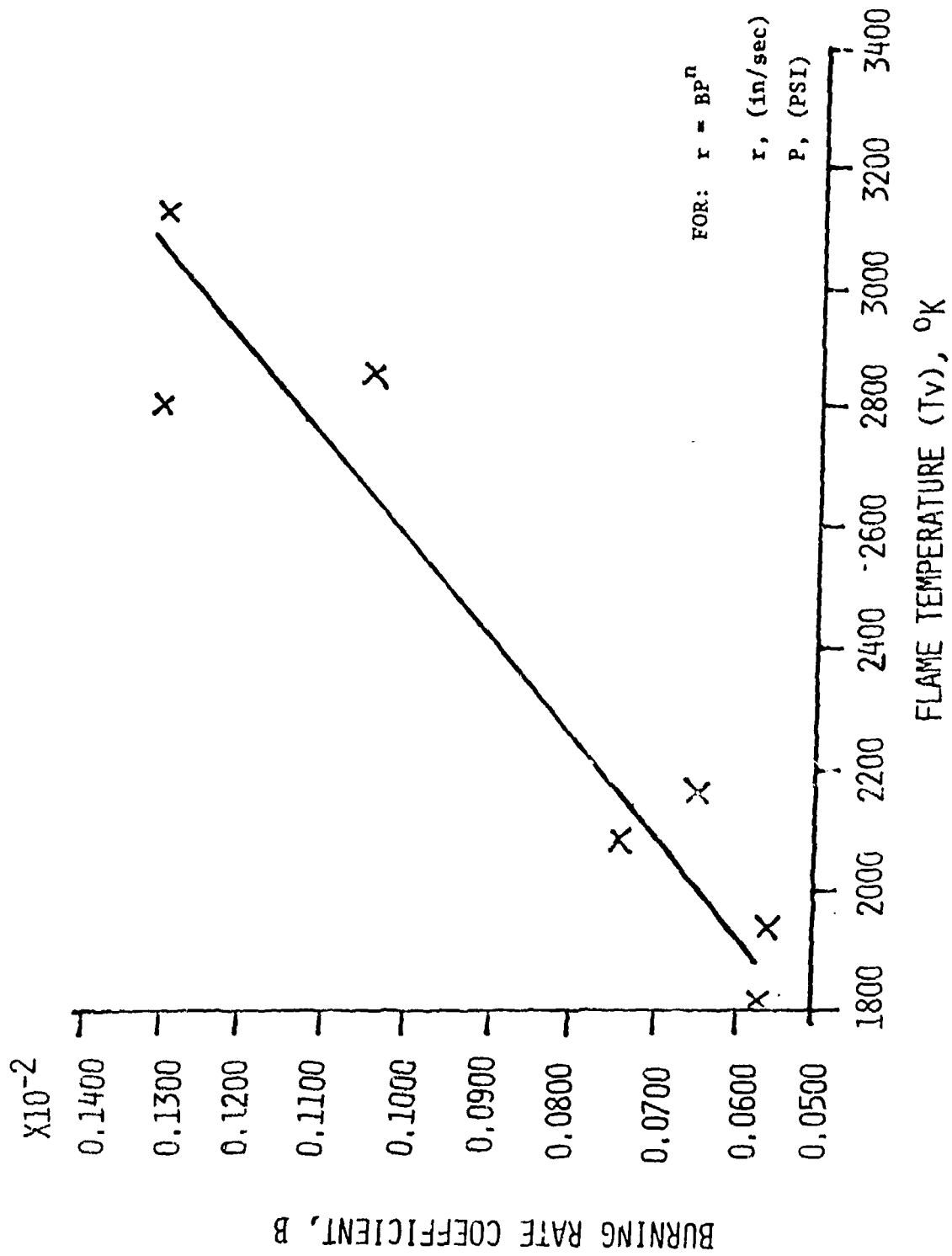


Figure 6. Correlation of burning rate with flame temperature, Riefler and Lowry data.

Table 12. Comparison of linear burning rates as estimated by various methods at 68.94 (10 Kpsi) and 137.9 MPa (20 Kpsi)

T <sub>0</sub> K	Burning Rate Exponent	Burning Rates (mm/sec)											
		GROLLMAN AND NELSON		MURAUOR		GOLDSTEIN		RIEFLER AND LOWERY A		RIEFLER AND LOWERY B			
		MPa	MPa	MPa	MPa	MPa	MPa	MPa	MPa	MPa	MPa	MPa	
3200	1	58.7	117.4	57.2	109.2	72.9	118.6	65.8	115.1	65.4	96.6		
3200	0.7												
2960	1	48.8	97.3	49.0	93.0	59.4	96.3			50.3	87.6		
2960	0.7												
2350	0.8	29.7	51.8	33.5	62.0	35.1	56.6			34.5	60.5		
2350	1												
2350	0.7												
2000	1	8.38	16.8	27.4	49.5	25.9	42.2	26.4	46.2	25.7	45.5		
2000	0.7												

Table 12. (Continued)

Tv K	Burnling Rate	GROLLMAN & NELSON		MARAOUR		GOLDSTEIN		RIEFLER AND LOWERY					
		Exponent	10 Kpsi	20 Kpsi	10 Kpsi	20 Kpsi	10 Kpsi	20 Kpsi	A	B	10 Kpsi	20 Kpsi	
3200	1	2.31	4.62	2.25	4.30	2.87	4.67	2.59	4.53	2.22	3.88		
3200	0.7											*	
2960	1	1.92	3.83	1.93	3.66							1.98	3.45
2960	.7					2.34	3.79						
2350	0.8	1.17	2.04										
2350	1			1.32	2.44							1.36	2.38
2350	0.7					1.38	2.23						
2000	1	0.33	0.66	1.08	1.95								
2000	0.7					1.02	1.66	1.04	1.82	1.01	1.79		

\*n = 0.8053

## RECOMMENDATIONS

1. The data base presented in this paper should be used in available computer codes for closed-bomb and gun interior ballistics.

2. Efforts should be made to further develop empirical burning rate correlations based on the flame temperature or on the heat of explosion to expand burning rate profile data for deterred propellants.

3. Further efforts should be made to refine interior ballistic codes that permit explicit inputs of thermochemical and burning rate properties of the various regions in small arms propellant grains.

## REFERENCES

1. T. R. Trafton, "An Improved Interior Ballistic Model for Small Arms Using Deterred Propellants," Ballistic Research Laboratories, APG Report No. 1264, November 1972.
2. F. Fortino, "Effect of Consolidation Parameters on the Burning of Consolidated Propellant Charges," 1979 JANNAF Propulsion Conference, 6-8 March 1979, Anaheim, California.
3. K. K. Kuo, R. Vichnevetsky, and M. Summerfield, "Theory of Flame Front Propagation in Porous Propellant Charges under Confinement," AIAA Journal, Volume II, No. 4, April 1973, pp 444-451.
4. S. Goldstein, "A Simplified Model for Predicting the Burning Rate and the Thermochemical Properties of Deterred Rolled Ball Propellant," Frankford Arsenal Technical Note TN-1184, December 1973.
5. M. E. Levy, "Microscopic Studies of Ball Propellant," Frankford Arsenal Report R-1286, September 1955.
6. M. E. Levy, "The Use of Deterrents in Small Arms Propellants - A Comprehensive Review," Frankford Arsenal Report FA-TR-76004, April 1976, pp 35-36.
7. "Autoradiographic Determination of Dibutyl Phthalate in Nitrocellulose Based Propellants," Olin Corporation Final Progress Report for Period 31 August - 30 November 1970, Contract LAAA-25-70-C-0140.

8. B. W. Brodman, M. P. Devine, R. W. Finch, and M. McLaren, "Autoradiographic Determination of Di-n-butyl Phthalate Concentration Profile in Nitrocellulose Matrix," Journal of Applied Polymer Science, 18, 12, December 1974, pp 3739-3744.
9. B. W. Brodman, J. A. Sipia, Jr., and S. Schwartz, "Diffusion of Deterrents into a Nitrocellulose Matrix. An Example of Diffusion with Interaction," Journal of Applied Polymer Science, Volume 19, 1975, pp 1905-1909.
10. J. Quinlan, "A Microscopic Examination of Extruded Double Base Propellants," Frankford Arsenal Report R-1302, December 1955.
11. J. Quinlan, "Microscopic Studies of Extruded Single Base Propellant," Frankford Arsenal Memorandum Report MR-623, April 1956.
12. F. Volk, "Konzentrationsverteilung von Oberflächenbehandlungsmitteln in Treibladungspulvern," (Concentration Gradient of Surface Treatment Agents in Propellants), Institut für Chemie der Treib- und Explosivstoffe (ICT), Bericht 1/73, 8 May 1973.
13. D. W. Riefler and D. J. Lowery, "Linear Burn Rates of Ball Propellants Based on Closed Bomb Firings," Olin Corporation, BRL Contractor Report No. 172, Contract DAAD05 73-C-0508, (August 1974).
14. S. Goldstein, "Burning Rate Model for Nondeterred Rolled Ball Propellant," Frankford Arsenal Technical Note TN-1144, February 1970.
15. S. Goldstein, "A Simplified Model for Predicting the Burning Rate and Thermochemical Properties of Deterred Rolled Ball Propellant," Frankford Arsenal Technical Note TN-1184, December 1973.
16. J.O. Hirshfelder and J. Sherman, "Simple Calculation of Thermochemical Properties for Use in Ballistics," National Defense Research Committee Report No. A-101 (OSRD Report 935), October 1943.
17. F. L. McMains, "Thermochemical Properties of Propellant Formulations by Means of a Computer Program," Picatinny Arsenal Technical Memorandum 1595, April 1965.

18. E. Freedman, "BLAKE - A Ballistic Thermodynamic Code Based on Tiger," Proceedings of the International Symposium on Gun Propellants, Picatinny Arsenal, 15-19 October 1973, pp 1.10-1 to 1.10-7.
19. B. B. Grollman and C. W. Nelson, "Burning Rates of Standard Army Propellants in Strand Burner and Closed Chamber Tests," 13th JANNAF Combustion Meeting, Naval Postgraduate School, Monterey, California, September, 1976, Volume 1, CPIA Publication 381, December 1976 pp 21-43.
20. H. Muraour, - as quoted by R. D. Geckler in "Selected Combustion Problems," AGARD, "The Mechanisms of Combustion of Solid Propellants," Butterworths, London, 1954, pp 289-299 (cited in reference 19 above).
21. "Solid Propellants: Part I, Engineering Design Handbook Ammunition and Explosive Series," U.S. Army Materiel Development and Readiness Command, DARCOM Pamphlet DARCOMP 706-175, 1964, p 14.

APPENDIX. SAMPLE CALCULATION FOR OBTAINING THE  
COMPOSITION OF THE DETERRED AND  
UNDETERRED REGIONS

Example: WC 846, LOT BAJ 45608

Composition as Reported on Description Sheet

Nitrocellulose (by difference)	82.42
% nitrogen in NC	(13.16)
Nitroglycerin	10.52
Dibutyl phthalate	5.68
Dinitrololuene	0.06
Diphenylamine	0.98
Total volatiles (T.V.)	1.23
Moisture and volatiles	1.06
Residual solvent	0.60
Calcium carbonate	0.13
Sodium sulfate	0.09
Graphite	0.12
	<u>101.23</u>

Note: All ingredients except graphite are reported by Badger AAP on a volatiles free basis. The reader is cautioned that the manner of reporting differs with different manufacturers.

1. To convert the reported percentages to percentage of the total propellant including total volatiles:

$$\text{fraction of ingredient } i \text{ on the total propellant basis} \times 100 = \frac{\text{fraction of ingredient } i \text{ on volatiles free basis}}{(A-1)} \times (100 - T.V.)$$

where T.V. = % total volatiles.

Example for nitroglycerin:

Let X = fraction of nitroglycerin on total propellant basis then from equation A-1.

$$X = \frac{0.1052(100-1.23)}{100}$$

$$X = 0.1039$$

$$0.1039 \times 100 = 10.39\% \text{ nitroglycerin total propellant basis.}$$

2. Composition of the WC 840 propellant on a total propellant basis is therefore:

<u>INGREDIENT</u>	<u>%</u>
Nitrocellulose	81.40
% nitrogen in NC	(13.16)
Nitroglycerin	10.39
Dibutyl phthalate	5.61
Dinitrotoluene	0.06
Diphenylamine	0.97
Total volatiles	(1.23)
Moisture	0.62
Residual solvent	0.61
Calcium carbonate	0.13
Sodium sulfate	0.09
Graphite	0.12
	<u>100.00</u>

3. For purposes of the thermochemical calculations, the total volatiles were arbitrarily split with half reported as moisture (H<sub>2</sub>O) and half as residual solvent (ethyl acetate). For single base propellants, the residual solvent is assumed to be ethyl alcohol.

4. No DBP is present in the undeterred region. To report the composition on a DBP free basis:

$$\text{fraction of ingredient } i \text{ in undeterred region} \times 100 - \% \text{DBP}^* = \frac{\text{fraction of ingredient } i \text{ in overall composition}}{\text{in overall composition}} \times 100 \quad (\text{A-2})$$

\*% DBP in overall composition

Example for nitroglycerin:

Let X - fraction of nitroglycerin in undeterred region.

Then from equation A-2,

$$X (100 - 5.61) = 0.1039(100)$$

$$X = \frac{0.1039(100)}{94.39} = 0.1101$$

and  $0.1101 \times 100 = 11.01\%$  = percentage of nitroglycerin in the undeterred region.

5. The composition of the undeterred region in the WC 846 propellant is:

<u>INGREDIENT</u>	<u>%</u>
Nitrocellulose	86.23
% nitrogen in NC	(13.16)
Nitroglycerin	11.00
Dibutyl phthalate	0.00
Dinitrololuene	0.06
Diphenylamine	1.02
Total volatiles	
Moisture	0.66
Residual solvent	0.65
Calcium carbonate	0.14
Sodium sulfate	0.10
Graphite	<u>0.13</u>
	100.00

6. As explained under the section of this report on thermochemical calculations, the measured depth of penetration was used to obtain the weight percent of the region containing deterrent. (For WC 846, this was 43.13%.)

Therefore, in 100 g of the WC 846 propellant, the deterrent containing region weighs 43.13 g.

Also, of 100 g of the WC 846 propellant, 5.61 g are dibutyl phthalate deterrent.

Since all of the deterrent is in the 43.13 g of deterrent-containing region, the concentration of DBP in that region is:

$$\frac{5.61}{43.13} \times 100 = 13.01\%$$

7. The deterrent-containing region contains all of the DBP; the other ingredients are present in the same proportion as in the undeterred region.

Therefore,

$$\text{fraction of ingredient } i \text{ in deterred region} \times 100 = \text{fraction of ingredient } i \text{ in the undeterred region} \times (100 - \% \text{DBP}^{**}) \quad (\text{A-3})$$

\*\*% DPB in the deterrent-containing region.

Example for nitroglycerin:

Let X = fraction of nitroglycerin in the deterred region.

Then,

$$X = \frac{0.1100(100-13.01)}{100}$$

$$X = 0.0957$$

and  $100(0.0957) = 9.57\%$  = percentage of nitroglycerin in the deterred region.

8. The composition of the deterrent containing region is:

<u>INGREDIENT</u>	<u>%</u>
Nitrocellulose	75.01
% nitrogen in NC	(13.16)
Nitroglycerin	9.57
Dibutyl phthalate	13.01
Dinitrotoluene	0.05
Diphenylamine	0.90
Total volatiles	
Moisture	0.57
Residual solvent	0.57
Calcium carbonate	0.12
Sodium sulfate	0.09
Graphite	0.11
	<u>100.00</u>

DISTRIBUTION LIST

Commander  
U.S. Army Materiel Development & Readiness Command  
ATTN: Technical Library  
Rock Island, IL 61299

Director  
Ballistic Research Laboratory  
U.S. Army ARRADCOM  
ATTN: Technical Library  
Aberdeen Proving Ground, MD 21005

Director  
Ballistic Research Laboratory  
U.S. Army ARRADCOM  
ATTN: I.W.May/DRDAR-BLP  
A.W.Barrows/DRDAR-BLP  
E.H.Freedman/DRDAR-BLP  
T.R.Trafton/DRDAR-BLP  
Aberdeen Proving Ground, MD 21005

Commander  
Air Force Armament Laboratory  
ATTN: Technical Library  
Eglin Air Force Base, FL 32542

Commander  
Air Force Armament Laboratory  
ATTN: B. May/AFATL-DL DL  
D. Davis/AFATL-DL DL  
Eglin Air Force Base, FL 32548

Commander  
U.S. Naval Surface Weapons Center  
ATTN: Technical Library  
Silver Spring, MD 20910

Commander  
U.S. Naval Ordnance Station  
ATTN: Technical Library  
Indian Head, MD 20640

Commander  
Radford Army Ammunition Plant  
ATTN: J. Horvath  
Radford, VA 24141

E.I. duPont de Nemours & Co.  
Explosive Products Division  
ATTN: L. Werner  
Wilmington, DE 19898

Weapon System Concept Team/CSL  
ATTN: DRDAR-ACW  
Aberdeen Proving Ground, MD 21010

Technical Library  
ATTN: DRDAR-CLJ-L  
Aberdeen Proving Ground, MD 21010

Technical Library  
ATTN: DRDAR-TSB-S  
Aberdeen Proving Ground, MD 21005

Benet Weapons Laboratory  
Technical Library  
ATTN: DRDAR-LCB-TL  
Watervliet, NY 12189

Commander  
U.S. Army Armament Materiel Readiness Command  
ATTN: DRSAR-LEP-L  
Rock Island, IL 61299

Director  
U.S. Army TRADOC Systems Analysis Activity  
ATTN: ATAA-SL (Tech Lib)  
White Sands Missile Range, NM 88002

Commander  
U.S. Army Materiel Systems Analysis Activity  
ATTN: DRXSY-MP  
Aberdeen Proving Ground, MD 21005

University of Illinois  
Dept of Aeronautical Engineering  
ATTN: Prof. H. Krier  
Urbana, IL 61801

Hercules, Incorporated  
ATTN: D. Mellow  
Kenvil, NJ 07847

Olin Corporation  
Smokeless Powder Operation  
ATTN: R. L. Cook  
P.O. Box 222  
St. Marks, FL 32355

Olin Corporation  
Military Marketing  
ATTN: H. F. Palmer  
East Alton, IL 62024

Defense Technical Information Center (12 cys)  
Cameron Station  
Alexandria, VA 22314

Commander  
U.S. Army Armament Research & Development Command  
ATTN: DRDAR-SCA, Dr. D. A. Gyrog  
C. J. Rhoades  
H. Kahn  
B. Brodman  
R. Fedyna  
L. Stiefel (10 cys)  
R. Udell  
R. Reagan  
S. Goldstein  
F. Fortino  
T. Hung  
DRDAR-LC, Dr. J. T. Frasier  
DRDAR-SCP  
DRDAR-TSS (5 cys)  
DRDAR-LCA-G, Dr. H. Fair  
E. Costa  
C. Lenchitz  
R. Trask  
DRDAR-LCE-D, Dr. J. Hershkowitz  
DRDAR-LCE, Mr. S. Bernstein  
Dr. J. Picard  
Dover, New Jersey 07801

Commander  
US Army Materiel Development and Readiness Command  
ATTN: DRCDMD, MG R. Baer  
DRCDMD-ST, N. Klein  
5001 Eisenhower Avenue  
Alexandria, VA 22333

Commander  
US Army Aviation Research and Development Command  
ATTN: DRSAV-E  
P.O. Box 209  
St. Louis, MO 63166

Director  
US Army Air Mobility Research and Development Laboratory  
Ames Research Center  
Moffett Field, CA 94035

Calspan Corporation  
ATTN: G. Sterbutzel  
F. Vassallo  
P.O. Box 235  
Buffalo, NY 14221

Director  
Chemical Propulsion Info Agency  
Johns Hopkins University  
ATTN: T. Christian  
Johns Hopkins Road  
Laurel, MD 20810

Physics Internation  
ATTN: Mr. Ron Brown  
San Leandro, CA 94577

Director  
US Army Research Office  
ATTN: P. Parrish  
E. Saibel  
P.O. Box 12211  
Research Triangle Park, NC 27709

Commander  
US Naval Surface Weapons Center  
ATTN: Jesse L. East, Jr., G-24  
Dahlgren, VA 22448

Commander  
US Naval Ordnance Station  
ATTN: L. Dickinson  
S. Mitchell  
C. Irish  
Indian Head, MD 20640

Office of Deputy Undersecretary  
of Defense, Research and Engineering  
The Pentagon  
ATTN: Mr. R. Thorkildsen, USDDR&E  
Room 3D1098  
Washington, D.C. 20301

Defense Advanced Research Projects Agency  
Director, Materials Division  
1400 Wilson Boulevard  
Arlington, VA 22209

Commander  
US Army Materiel Development and Readiness Command  
ATTN: DRCDMD-CT  
5001 Eisenhower Avenue  
Alexandria, VA 22333

HQDA  
ATTN: SAUS-OR, D. Hardison  
Washington, DC 20310

HQDA  
ATTN: DAMA, LTC H. Glock  
Washington, DC 20310

Battelle Columbus Laboratories  
ATTN: Dr. D. Trott  
505 King Avenue  
Columbus, OH 43201

Calspan Corporation  
ATTN: Mr. E. B. Fisher  
P.O. Box 235  
Buffalo, NY 14221

Shock Hydrodynamics, Inc.  
ATTN: Dr. H. Anderson  
4710-16 Vineland Avenue  
N. Hollywood, CA 91602

Thiokol, Wasatch Division  
ATTN: Dr. F. Bell  
P.O. Box 524  
Brigham City, UT 84302

Pennsylvania State University  
Dept. of Mechanical Engineering  
ATTN: Prof. K. Kuc  
University Park, PA 16802

A. Buckingham  
Lawrence Livermore Laboratories  
University of California  
Livermore, CA 94550

Aerojet Ordnance and Manufacturing Co.  
ATTN: Technical Library  
9236 E. Hall Road  
Downey, CA 90241

Honeywell  
Defense Systems Division  
ATTN: Technical Library  
600 Second Street, NE  
Hopkins, MN 55343

Ford Aerospace & Communications Division  
Aeroneutronics Division  
Ordnance Systems  
ATTN: Technical Library  
Newport Beach, CA 92663

ERRATA

Technical Report ARSCD-TR-80005

THERMOCHEMICAL AND BURNING RATE  
PROPERTIES OF  
DEFERRED US SMALL ARMS PROPELLANT

Ludwig Stiefel

June 1980

Equation 3 on page 15 was in error and has been corrected. Remove pages 15 and 16, therefore, and insert attached revised pages 15 and 16.

2 September 1980

80 9 29 094

AD A086093

The average volume of the rolled-ball grains is given by:

$$\bar{V}_o = 2\pi r (\bar{R}-r)^2 + \pi^2 r^2 \left[ (\bar{R}-r) + \frac{4}{3} \frac{r}{\pi} \right] \quad (3)$$

The value for  $D_o^{(S)}$  was obtained by inserting the appropriate number into equation 1. For the WC 846 propellant lot BAJ 45608,  $D_o^{(S)} = 0.5473$  mm.

If the depth of penetration of deterrent is  $x$ , the volume of the undeterred region  $V_{un}$  is:

$$V_{un} = 2\pi(\bar{R}-r)^2(r-x) + \pi^2(r-x)^2 \left[ (\bar{R}-r) + \frac{4(r-x)}{3\pi} \right] \quad (4)$$

The total grain volume  $\bar{V}_o$  was found to be  $0.0670 \text{ mm}^3$ , and the volume of the undeterred larger  $\bar{V}_{un}$  was found to be  $0.0381 \text{ mm}$  (ref 3). Then, the undeterred region occupies:

$$\frac{\bar{V}_{un}}{\bar{V}_o} \times 100 = 56.87\% \text{ of the volume of the grain.}$$

On the assumption that all of the deterrent, DBP, i.e., 5.28 percent (table 2) was located in the deterred region, the concentration of that region was found to be 12.24 percent. The composition of the deterred and undeterred regions was then calculated and is given in table 6 along with the overall composition given in table 2. Details of this part of the calculation are given in the appendix.

The values for moisture ( $H_2O$ ) and residual solvent have been arbitrarily taken to be equal to one-half of the total volatiles in the following tables. This was done because the reported values for moisture are obtained by empirical methods and the validity is questionable.

Calculation of the composition of the deterrent-containing and undeterred region of the spherical ball propellant (unrolled) WC 870 follows the same procedure, except that the geometry of the grain is assumed to be a sphere which simplifies the applicable equations (i.e., equations 2, 3, and 4) accordingly.

The weighted mean diameter based on surface area  $D_o^{(S)}$  of the grain of WC 870 Lot A.L. 45137 was found to be 0.7902 mm. The average grain volume,  $\bar{V}$ , was  $2.584 \times 10^{-4} \text{ cm}^3$ . The average volume of the undeterred region,  $\bar{V}_{un}$ , was found to be  $1.649 \times 10^{-4} \text{ cm}^3$  and the undeterred region in the WC 870 propellant was found to occupy 63.79 percent of the total volume of the grain. The compositions of the deterred and undeterred layers determined from these results are given in table 5.

The extruded propellants have a uniform grain geometry (i.e., single perforated cylinders) as given in table 3. Calculation of the composition of the deterred and undeterred regions for these propellants involves the following steps:

1. Calculate the volume of the total grain.
2. Calculate the volume of the deterred region using the measured depths of deterrent penetration in table 4.
3. Assuming that all of the deterrent is concentrated in the deterred region, calculate the concentration of the deterrent in that region. Then, obtain the concentrations of the other constituents.
4. Assuming total absence of the deterrent in the undeterred region, calculate its composition.

The results of these computations for the extruded propellants are given in tables 8 and 9, along with their overall chemical composition. For purposes of comparison, the percentage of the propellant grain volume, occupied by the deterrent-containing region for each of the propellants is listed in table 10.

Two methods were used for calculating the thermochemical properties associated with the compositions given in tables 6, 7, 8, and 9 were used. One of these was the Hirshfelder-Sherman Additive Constant method (ref 16). A computer program (ref 17) based on this method, was used for these calculations.